Published in final edited form as:

Cancer Immunol Res. 2021 August ; 9(8): 952–966. doi:10.1158/2326-6066.CIR-20-0834.

ST8Sia6 Promotes Tumor Growth in Mice by Inhibiting Immune Responses

David J. Friedman[1], **Sydney B. Crotts**[1], **Michael J. Shapiro**[1], **Matthew Rajcula**[1], **Shaylene McCue**[1], **Xin Liu**[1], **Khashayarsha Khazaie**[1], **Haidong Dong**[1,2], **Virginia Smith Shapiro**[1,*]

[1]Department of Immunology, Mayo Clinic; Rochester, MN, 55905, USA

[2]Department of Urology, College of Medicine, Mayo Clinic; Rochester, MN, 55905, USA

Abstract

Many tumors exhibit increased incorporation of sialic acids into cell-surface glycans, which impact the tumor microenvironment. Sialic acid immunoglobulin-like lectins (Siglecs) are receptors that recognize sialic acids and modulate immune responses, including responses to tumors. However, the roles of individual sialyltransferases in tumorigenesis and tumor growth is not well understood. Here, we examined the sialyltransferase, ST8Sia6, which generated α2,8-linked disialic acids that bind to murine Siglec-E and human Siglec-7 and -9. Increased ST8Sia6 expression was found on many human tumors and associated with decreased survival in several cancers, including colon cancer. Because of this, we engineered MC38 and B16-F10 tumor lines to express ST8Sia6. ST8Sia6-expressing MC38 and B16-F10 tumors exhibited faster growth and led to decreased survival, which required host Siglec-E. ST8Sia6 expression on tumors also altered macrophage polarization towards M2, including upregulation of the immune modulator arginase, which also required Siglec-E. ST8Sia6 also accelerated tumorigenesis in a genetically engineered, spontaneous murine model of colon cancer, decreasing survival from approximately 6 months to 67 days. Thus, ST8Sia6 expression on tumors inhibits antitumor immune responses to accelerate tumor growth.

Keywords

Cancer; Immunology; Glycobiology; Innate Immunity; Macrophages

Introduction

Checkpoint immunotherapy has made major strides in the treatment of cancer. Approved therapies, such as anti-PD-1, anti-PD-L1, and anti-CTLA-4, have improved patient outcomes in melanoma and lung cancer (1-2). The clinical success of these inhibitors demonstrates the critical role that the immune system plays in eliminating cancer. However,

[*]**To whom all correspondence should be addressed:** Virginia Smith Shapiro, Ph.D., Department of Immunology, 4-01 C Guggenheim Building, Mayo Clinic, 200 First Street SW, Rochester, MN 55905, Phone: 507-293-0615, Fax: 507-284-1637, Shapiro.Virginia1@mayo.edu.

Conflict of interest:
The authors have declared that no conflict of interest exists.

these therapies primarily function by modulating T-cell activation (3). Unfortunately, many patients do not respond to checkpoint inhibitors, demonstrating that these tumors may be targeting different cellular components of the immune response, such as the CD47 “don’t eat me” signal (4). Cancer cells also modulate immune responses by promoting the differentiation of macrophages recruited into the tumor into pro-tolerogenic, M2 tumor-associated macrophages (TAMs)(5) or myeloid-derived suppressor cells (MDSCs) (6). Many tumors exhibit increased incorporation of sialic acids into cell surface glycans, which can engage sialic acid immunoglobulin-like lectins (Siglecs) (7-8).

Siglecs are a family of transmembrane proteins expressed primarily on hematopoietic cells and regulate immune activation (9). Siglecs are generally divided into two families, which are either structurally conserved across species (including Siglec-1, -2, -4, and -15) or divergent (CD33-related Siglecs). There is not a strict one-to-one correlation of CD33-related Siglecs between species (9). Thus, human CD33-related Siglecs are designated with numbers, whereas murine CD33-related Siglecs are designated with letters. Many, but not all, Siglecs contain an intracellular immunoreceptor tyrosine-based inhibitory motif (ITIM) in their cytoplasmic tails. ITIMs function by recruiting tyrosine phosphatases, such as SHP1 and SHP2, to dampen immune cell activation. Siglecs recognize ligands that contain sialic acids, with each having a preference for the type/linkage of sialic acid for which they recognize (10). Siglecs have also been shown to regulate immune responses to cancer. For example, sialylated CD24 sends an inhibitory signal through Siglec-10 to block phagocytosis and macrophage activation (11), Siglec-15 blockade enhances tumor responses in mouse models (12), and Siglec-9 engagement on neutrophils inhibits tumor killing (13). Siglec-E is most closely related to Siglec-9 by sequence in humans, and Siglec-E knockout mice have enhanced anti-tumor immune responses (13). Targeting Siglec-E ligands on tumor cells has been shown to be an effective immunotherapy in mice (14). Although a role for Siglecs in modulating immune responses has been identified, the role of individual sialic acid transferases in protecting tumors from the immune response is largely uncharacterized.

Sialic acids are 9-carbon monosaccharides found at the termini of cell surface glycans, both glycoproteins and glycolipids. Sialic acid can be added to glycans by one of three linkages, differentially named for the carbon atom in the terminal sugar which is used to attach it to the sialic acid (α2,3, α2,6 or α2,8) by one of twenty sialic acid transferases. Siglec-E preferentially binds to α2,8-linked disialic acids, as compared to either α2,3 or α2,6 linked sialic acids (15). There are six sialyltransferases that generate α2,8 linked sialic acids – ST8Sia1-6. However, only ST8Sia6 generates disialic acids, adding a single α2,8 linked sialic acid onto an existing α2,3 or α2,6 linked sialic acid (16). We previously demonstrated that the sialyltransferase ST8Sia6 generates ligands for Siglec-E *in vivo* (17). Because Siglec-E has been shown to modulate immune responses to tumors in mice, we asked whether ST8Sia6 expression in tumors could inhibit the immune response.

Here, we analyzed the function of ST8Sia6 overexpression in regulating antitumor immune responses. Examination of public databases demonstrated that ST8Sia6 was overexpressed in human cancers, and in a subset of tumors, associated with worse survival. The well-characterized MC38 and B16-F10 tumor cells do not express detectable levels of ST8Sia6, and we engineered paired cell lines with and without ST8Sia6 expression to directly

examine its role in tumor growth. Stable expression of ST8Sia6 generated ligands for murine Siglec-E, as well as human Siglec-7 and -9, demonstrating that ST8Sia6 generates ligands for Siglec-7 and -9. In syngeneic C57Bl/6 mice, MC38 and B16-F10 tumors overexpressing ST8Sia6 exhibited significantly increased tumor growth compared to controls. This increase in tumor burden was dependent on host Siglec-E expression because the growth advantage of ST8Sia6-expressing MC38 and B16-F10 cells was lost when injected into Siglec-E knockout (KO) mice. Examination of tumor-infiltrating immune cells demonstrated that Siglec-E expression was restricted to innate immune cells and was not expressed by T cells. ST8Sia6 did not alter the number of infiltrating immune cells into tumors. However, ST8Sia6 expression on tumors altered polarization of macrophages, leading to increased arginase-1 (Arg-1) protein expression, which associated with an M2-like/alternatively activated macrophage phenotype. This increase in Arg-1 depended on Siglec-E expression on macrophages. We also generated a spontaneous mouse model of colon cancer, in which we demonstrated that increased ST8Sia6 expression accelerated tumorigenesis, leading to a reduction in survival from a median of approximately 6 months to only 67 days. Thus, ST8Sia6-mediated modifications are a mechanism to modulate immune responses, promoting tumor growth and development.

Materials and Methods

Cell lines

The MC38 murine colorectal cancer cell line was received from Dr. Yang-Xin Fu (UT Southwestern Medical Center, Dallas, Texas) (18), and the B16-F10 murine melanoma cell line was purchased from ATCC (Cat. #CRL-6475). Cell lines were screened for Mycoplasma contamination and authenticated by STR profiling (B16 at ATCC and MC38 at IDEXX). PD-L1 knockout (KO) MC38 and B16-F10 cell lines were generated by knocking out mouse B7-H1 by CRISPR/Cas9 technology. The guide sequence (5'-GTATGGCAGCAACGTCACGA-3') specific to mouse B7-H1 exon 3 (the second coding exon) was designed using the CRISPR DESIGN tool (http://crispr.mit.edu) and cloned into the px458 plasmid co-expressing GFP (Addgene, #52961). Thirty-six hours after transfection, CRISPR/Cas9-expressing cells were single-cell subcloned using flow cytometry sorting for GFP expression and further expanded for genotyping using PCR for knockout validation and Western blotting for B7-H1 protein depletion. Cell lines were cultured in RMPI 1640 (Cat. #10-040-CV, Corning) supplemented with 10% fetal bovine serum (Cat. #SH30910.03, HyClone), 1% penicillin/streptomycin solution (Cat. #15140-122, Gibco), 1% L-glutamine 200mM (100X; Cat. 25030-081, Gibco), 1% sodium pyruvate (Cat. #25-000-CI, Corning), 1% HEPES (1M) (Cat. #15630-080, Gibco), and 1% MEM nonessential amino acids (Cat. #25-025-CI, Corning). Cells were passaged using 0.25% Trypsin-EDTA (1X) (Cat. #25200-056, Gibco) every 2 to 3 days. Cells were passaged no more than 10 times for use before new stocks were cultured.

Animals

C57Bl/6 (Stock #000664) and LNL-tTA (Stock #008600) mice were obtained from JAX. Siglec-E KO mice (Stock #032571-UCD) were obtained from the Mutant Mouse Resource and Research Center (US Davis, Davis, CA). Experiments were conducted on both male and

female mice that were between 6 to 8 weeks of age. Tumor growth and survival experiments were performed with 4 to 6 mice per group, and tumor harvest experiments were performed with 4-5 mice per group. Ts4-cre $APC^{lox468(fl/wt)}$ $LSLKras^{G12D}$ (TAR) mice are previously described (19). ST8Sia6 LNL-tTA Ts4-cre $APC^{lox468(fl/wt)}$ $LSLKras^{G12D}$ (StTAR) mice were developed in collaboration with the Mayo Clinic Transgenic and Knockout Mouse Core Facility. Briefly, Myc-tagged ST8Sia6 (generation described below) was inserted into an expression cassette within the ColA1 safe harbor locus utilizing FLP recombinase in KH2 ES cells to allow for its induction in cre-expressing cells as published (20). The generation of mice utilizing this knock-in system has been previously described (17). These mice were then crossed with TAR mice to generate StTAR mice. All mouse work was performed with approval from the Mayo Clinic Institutional Animal Care and Use Committee.

Construction of Myc-tagged ST8Sia6 expression plasmid

A plasmid containing the complete coding sequence of murine ST8Sia6 was purchased from Open Biosystems (clone 40104779). PCR was used to amplify the ST8Sia6 gene (Forward primer sequence: GCGGATCCGTGGCTCAGGATGAGATCGGG; Reverse primer sequence: GCGCGGCCGCGCAGCCGTTTCACATTTGCTGAATTG) and incorporate BamHI and NotI restriction sites on the 5’ and 3’ ends, respectively. The PCR product was subcloned into the pEF6/Myc-His(A) plasmid (Invitrogen) to create an expression vector with an in-frame Myc-His epitope at the C-terminus. The insert was sequenced to ensure the absence of unintended mutations.

Transfection of cell lines

Both ST8Sia6-Myc containing and empty vector control plasmids were transfected into both MC38 and B16-F10 utilizing FuGENE 6 transfection reagent (Cat. #E2691, Promega) according to the manufacturer’s instructions. Cells were incubated at 37°C for 24 hours and then blasticidin (10μg/mL; Cat. #15205, Sigma Aldrich) was added to the media to select for clones. Once individual colonies had formed, they were picked and expanded in complete media as outlined above supplemented with blasticidin (10μg/mL) until colonies were 50% confluent in 24-well plates. Media was replaced on the cells with fixation buffer, which consisted of 37% formalin (Cat. #, COMPANY) diluted 1:10 in 1X $PBS^{-/-}$ (Cat. #21-040-CV, Corning). Colonies were incubated in fixation buffer for 15 minutes at room temperature and then washed with $PBS^{-/-}$. Cells were incubated in Perm/Block for 1 hour, which consisted of 5% normal goat serum (50062Z, Life Technologies), 0.3% Triton X-100 (Cat. #BP151-100, Fisher BioReagents), and $PBS^{-/-}$. Cells were washed in dilution buffer, which consisted of $PBS^{-/-}$, 0.3% Triton X-100, and 1% BSA (Cat. #3116964001, Sigma Aldrich). Cells were stained using a primary antibody against the Myc-tag (Cat. # 2276S, Cell Signaling) in dilution buffer overnight at 4°C. Cells were washed in dilution buffer and stained using the secondary antibody, goat ant-mouse IgG-AF488 (Cat. #A11029, Invitrogen), in dilution buffer for 1 hour at room temperature. Cells were washed in dilution buffer and screened for ST8Sia6-Myc expression by immunofluorescence using the Leica DMI3000B.

MC38 or B16-F10 cells that stably expressed ST8Sia6-Myc were additionally screened for the generation of Siglec-E ligands using recombinant Siglec-E (Cat. #551506, BioLegend).

Cells were plated into 96-well plates at 5 x 10^6 cells per well and blocked in rat serum (Cat. #10710C, Invitrogen) for 10 minutes on ice and subsequently stained using recombinant Siglec-E for 30 minutes. Cells were washed with PBS (Cat. #21-030-CV, Corning) and stained with the secondary antibody goat anti-human IgG-PE (Cat. #109-115-098, Jackson ImmunoResearch Laboratories). Cells were washed with PBS and analyzed using the Attune NxT flow cytometer (Life Technologies). This process was repeated in PD-L1 KO MC38 and B16-F10 cell lines. A pCDNA3.1(+)-C-Myc expression plasmid encoding murine CMAH was purchased from GenScript (OMu00672C). 293T cells were transfected with Fugene6 reagent (Promega) according to the manufacturer's instructions. For each experiment, cells plated in a 10 cm dish were transfected with a cocktail containing 30 μL of Fugene6 reagent and either no expression plasmid, 5 μg of St8Sia6 expression plasmid, 5 μg of CMAH expression plasmid, or 5 μg of both expression plasmids. Empty vector was added as necessary so that each cocktail contained 10 μg total DNA. 48 hours after the start of transfection, cells were harvested by pipetting into suspensions and analyzed by flow cytometry.

Tumor models

5 x 10^5 cells were inoculated in the right flank of C57Bl/6 or Siglec-E KO mice for single injections or in both the left and right flanks for dual injections. Tumor were allowed to grow for 7 or 14 days and then either harvested for analysis (outlined in the tissue dissociation and flow cytometry sections) or followed for growth kinetics and survival. Tumor growth was monitored three times per week using calipers (Cat. # S90187A, Fisher Scientific) measuring length and width of each tumor. Once the total tumor burden reached 10% of the mouse body weight, mice were euthanized. Tumor volumes were calculated based using the equation volume = length (mm) x width2 (mm) x $\pi/6$.

Antibodies and reagents

Fluorescently conjugated antibodies CD45.2-BV785 (Cat. #109839, BioLegend), CD45.2-FITC (Cat. #109806, BioLegend), CD11b-FITC (Cat. #101206, BioLegend), CD11c-PE (Cat. #117308, BioLegend), CD11c-PE-Cy7 (Cat. #117324, BioLegend), F4/80-PE-Dazzle 594 (Cat. #123146, BioLegend), F4/80-BV421 (Cat. #123132, BioLegend), Ly6C-PerCP (Cat. #128028, BioLegend), Ly6G-BV510 (Cat. #127633, BioLegend), Ly6G-APC (Cat. #127614, BioLegend), IA/IE (MHC Class II)-BV605 (Cat. #107639, BioLegend), Recombinant Siglec-E-Fc (Cat. #551506, BioLegend), Streptavidin-PE-Cy7 (Cat. #405206, BioLegend), CD4-PerCP (Cat. #100538, BioLegend), CD8α-BV510 (Cat. #100752, BioLegend), CD25-BV785 (Cat. #102034, BioLegend), PD-1-FITC (Cat. #135214, BioLegend), LAG3-BV421 (Cat. #125221, BioLegend), TIM3-PE-Dazzle 594 (Cat. #134014, BioLegend), Siglec-E-APC (Cat. #677106, BioLegend), Siglec-E PE-Cy7 (Cat. #677108, BioLegend), and CD206-PE-Cy7 (Cat. #141720, BioLegend) were purchased from BioLegend. The antibody for TOX-PE (Cat. #12-6502-82, eBioscience) was purchased from eBioscence, anti-CD38-BV421 (Cat. #562768, BD Horizon) was purchased from BD Horizon, and anti-TCF1-AF647 (Cat. #6709S, Cell Signaling Technologies) was purchased from Cell Signaling Technologies. Fixable viability dye Ghost Red 780 (Cat. #13-0865-T100, Tonbo), anti-TCRβ-PE-Cy7 (Cat. #60-5961-U100, Tonbo), and anti-Foxp3-PE (Cat. #50-5773-U100, Tonbo) were purchased from Tonbo Biosciences. Recombinant Siglec-9-Fc

(Cat. #1139-SL, R&D Systems) and recombinant Siglec-7-Fc (Cat. #1138-SL, R&D Systems) were purchased from R&D Systems. Anti-human IgG-PE (Cat. #109-115-098, Jackson ImmunoResearch Laboratories) was purchased from Jackson ImmunoResearch Laboratories. SNBL-Biotin (Cat. #B-1305, Vector Laboratories) and MALII-Biotin (Cat. #B-1265, Vector Laboratories) were purchased from Vector Laboratories. Arg-1-APC (Cat. #12-3697-82, Invitrogen) and iNOS-PE (Cat. #17-5920-82, Invitrogen) were purchased from Invitrogen. Immunohistochemistry antibodies for PCNA (Cat. #13110S, Cell Signaling Technologies), αSMA (Cat. #19245S, Cell Signaling Technologies), and Arg-1 (Cat. #93668S, Cell Signaling Technologies) were purchased from Cell Signaling Technologies, and anti-MCM6 (Cat. #ab190948, Abcam) was purchased from Abcam. Anti-rabbit-HRP (Cat. #RMR622L, Biocare Medical) was purchased from Biocare Medical. The Western blot antibody for the Myc-tag (Cat. #2278S, Cell Signaling Technologies) was purchased from Cell Signaling Technologies, and the secondary antibody goat anti-rabbit IgG-HRP (Cat. #4050-05, Southern Biotech) was purchased from Southern Biotech.

Immunohistochemistry

For immunohistochemistry, murine colons were fixed in 10% formalin for 18-24 hours. Tissues were then processed for paraffin-embedded tissue sections. Paraffin-embedded tissues were cut in five-micrometer sections and mounted onto positively charged frosted slides for analysis. For H&E staining, tissue sections were deparaffinized and rehydrated before hematoxylin and subsequent eosin staining. Primary antibody staining for PCNA, MCM6, αSMA, and Arg-1 were carried out after antigen retrieval was performed using 1X citrate buffer at a of pH 6 (Cat. #C9999-1000ML, Sigma Aldrich) in a steamer (Cat. #HS1050, Black & Decker). Antibody binding was detected using rabbit-HRP secondary antibodies with DAB as the enzyme substrate. Sections were counterstained with hematoxylin and dehydrated before mounting the slides with permount for analysis. Images were obtained using a Leica DMI3000B microscope and analyzed using the Leica LAS EZ software. All images displayed are representative of the mouse phenotype at the age range indicated.

Tissue dissociation

Spleens were dissociated via manual disruption by placing each organ between two frosted microscope slides. The contents were filtered through 90μm Nitex nylon mesh (Cat. #B0013NHZAQ, Sefar America) in PBS. Samples were pelleted and incubated for 1-2 minutes in 1 mL of Ack Lysis buffer (Cat. #118-156-101, Quality Biological). Samples were washed in PBS and adjusted to 2.5 x 10^7 per mL. Tumors were manually dissociated using surgical scissors (Cat. #14060-10, Fine Science Tools), and the contents were digested in 1X collagenase cocktail in PBS (diluted from a 20X concentration), which consisted of collagenase from Clostridium histolyticum (Cat. #C5138-1G, Sigma Aldrich), deoxyribonuclease I from bovine pancreas (Cat. #D5025-15KU, Sigma Aldrich), hyaluronidase from sheep testes (Cat. #H6254-500MG, Sigma Aldrich) in PBS. Dissociated tumors in collagenase cocktail were shaken at 37°C for 45 minutes. Samples were washed in PBS, and total contents were stained for flow cytometry. Colons were cleaned using PBS in a 10 mL syringe with an animal feeding needle (Cat. #7903, Cadence Science) attached. Colons were placed on bibulous paper (Cat. #11-998, Fisher Scientific) and cut open

lengthwise using blunt-tipped scissors (Cat. #RS-5998, ROBOZ). Visible tumors were removed using surgical scissors. Tumors and colons were dissociated independently using surgical scissors and digested in 1X collagenase cocktail in complete media. Dissociated tumors and colons in collagenase cocktail were shaken at 37°C for 25 minutes. Digested contents were filtered through 70μm cell strainers (Cat. #22-363-548, Fisher Scientific) and washed in PBS. Total contents were stained for flow cytometry.

Flow cytometry

Total cellular contents were plated into 96-well plates for flank tumors, colons, and colonic tumors. Spleens were plated at 5 x 10^6 cells per well into a 96-well plate. Cells were blocked in a 1:1 mixture of mouse serum (Cat. #10410, Invitrogen) and rat serum (Cat. #10710C, Invitrogen) for 10 minutes on ice and subsequently stained with cell surface antibodies in PBS for 30 minutes on ice. Cells were washed with PBS (Cat. #21-030-CV, Corning) and fixed using Foxp3 Transcription Factor Fix/Perm Concentrate (4X) (Cat. #TNB-1020-L050, Tonbo Biosciences) diluted in Foxp3 Transcription Factor Fix/Perm Diluent (1X) (Cat. #TNB-1022-L160, Tonbo Biosciences) for 20 minutes on ice. Cells were washed with Flow Cytometry Perm Buffer (10X) (Cat. #TNB-1213-L150, Tonbo Biosciences) diluted in water. Cells were stained with intracellular antibodies in Perm Buffer for 30 minutes on ice. Cells were washed with PBS and analyzed using the Attune NxT flow cytometer (Life Technologies).

Western blots

Lysates were generated from HEK293T cells either transfected with EV, ST8Sia6, CMAH, or CMAH and ST8Sia6. Cells were resuspended in a buffer containing 50 mM Tris Base, pH 7.0 (Cat. #BP152, Fisher), 2% SDS (Cat. #BR161-0302, Bio-Rad), 10% glycerol (Cat. #G33, Fisher), 0.01% bromophenol blue (Cat. #BP115, Fisher), and 100 mM DTT (Cat. #D0632, Sigma). Cells were lysed using a 27-gauge needle and incubated at 95°C for 5 minutes. Lysates along with a ladder (Cat. #161-0305, Bio-Rad) were resolved on gels containing 375 mM Tris Base, pH 8.8, 0.1% SDS, 10% acrylamide (Cat. #1610156, Bio-Rad), 0.06% APS (Cat. #A3678, Sigma), and 0.1% TEMED (Cat. #161-0800, Bio-Rad). Gels were run using the Mini-PROTEAN Tetra System (Cat. #12-0625, Bio-Rad) at 150V for 1 hour using a buffer containing 25 mM Tris Base, 192 mM glycine (Cat. #BP381, Fisher), and 0.1% SDS. Protein was transferred to Immobilon-P membranes (Cat. #IPVH00010, Millipore) stacked with blotting paper (Cat.# 3030-392, Whatman) soaked in a buffer containing 48 mM Tris Base, 38 mM glycine, 0.04% SDS, and 20% methanol (Cat. #A452, Fisher) using a semi-dry transfer apparatus (Cat. #Z340502, Sigma) at 150 mA for 1 hour. Membranes were washed in TBST, which consisted of 1X TBS (Cat. #1706435, Bio-Rad), and 0.1% Tween 20 (Cat. # 1706531, Bio-Rad). Membranes were incubated in western block for 1 hour, which consisted of TBST supplemented with 3% BSA and then incubated with anti-Myc-tag antibody (Cat. #2278S, Cell Signaling Technologies) diluted 1:1000 in western block overnight at 4°C. Membranes were washed in TBST and incubated with goat anti-rabbit IgG-HRP (Cat. #4050-05, Southern Biotech) diluted 1:10,000 in western block for 1 hour. Membranes were washed with TBST and then coated with developing reagent (Cat. #NEL121001, Perkin Elmer) before exposure to film (Cat. #1141J52, Thomas Scientific).

RNA Isolation and qPCR for sialyltransferases

Total RNA was isolated from MC38 and B16-F10 cell lines using the RNeasy Mini Kit (Qiagen). RNA from a naïve C57Bl/6 spleen was used as a positive control. cDNA was generated from RNA using the SuperScript™ III First-Strand Synthesis System (Life Technologies). qPCR was conducted using the TaqMan™ Universal PCR Master Mix Kit (Life Technologies) and Taqman probes for murine ST3GAL1 (Mm_00501493), ST3GAL2 (Mm_00486123), ST3GAL3 (Mm_00493353), ST3GAL4 (Mm_00501503), ST3GAL5 (Mm_00488237), ST3AL6 (Mm_00450674), ST6GAL1 (Mm_00486119), ST6GAL2 (Mm_00555908), ST6GALNAC1 (Mm_01252949), ST6GALNAC2 (Mm_00486130), ST6GALNAC3 (Mm_01316813), ST6GALNAC 4 (Mm_01329921), ST6GALNAC5 (Mm_00488855), ST6GALNAC6 (Mm_00489927), ST8SIA1 (Mm_00456915), ST8SIA2 (Mm_01311039), ST8SIA3 (Mm_00456296), ST8SIA4 (Mm_01292231), ST8SIA5 (Mm_00457285), ST8SIA6 (Mm_00461200) in order to screen for mRNA expression, using 18S rRNA (4352930) from Applied Biosystems as a control. Samples were analyzed using the StepOnePlus Real-Time PCR System (Cat. #4376600, Applied Biosystems). Relative expression was calculated using ΔΔCt method.

Dataset analysis

Data were assembled and collated from the COSMIC database (https://cancer.sanger.ac.uk/cosmic) to examine changes in gene expression in published RNAseq studies. The definition for COSMIC to determine if a gene is overexpressed or underexpressed was a z score of greater than 2 or less than −2, meaning two standard deviations below or above the mean was considered as significant. COSMIC assembles data based on tumor location, and thus this represents mixed tumor and cell types. Tumor sites were annotated as follows: adrenal, breast, CNS, cervix, endometrium, hematopoietic/lymphoid, kidney, large intestine, liver, lung, esophagus, ovary, pancreas, prostate, skin, soft tissue, stomach, thyroid, upper digestive tract, and urinary tract. The analysis of patient outcome utilized the Human Protein Atlas (https://www.proteinatlas.org). The analysis used optimal difference between survival above (high) and below (low) a certain threshold of RNA expression based on FPKM (fragments per kilobase of transcript per mission mapped reads) as denoted figure legends. This data was extracted on 7-29-18. Data from the survival curves consisted of 597 patients in colon cancer (low ST8Sia6: 353, high ST8Sia6: 244), 354 patients in stomach cancer (low ST8Sia6: 267, high ST8Sia6: 87), 391 patients in cervical cancer (low ST8Sia6: 255, high ST8Sia6: 66), and 406 patients in urothelial cancer (low ST8Sia6: 310, high ST8Sia6: 96). The log-ranked p values from the Kaplan-Meier plot correlating mRNA expression and survival were provided with the survival analysis by the Human Protein Atlas.

Statistics

Data were graphed and analyzed using Prism (GraphPad Software). Tumor growth kinetics were compared using a two-way ANOVA with multiple comparisons, while survival data was assessed using a Mantel-Cox test. Individual parameter datasets across multiple groups were compared using a one-way ANOVA with multiple comparisons. Error bars represent SEM.

Results

ST8Sia6 is upregulated in human cancers and associates with poor survival in a subset of patients

Sialyltransferase expression in human cancers was examined using the COSMIC database (https://cancer.sanger.ac.uk/cosmic). The COSMIC database examines gene expression based on organ, and not on individual tumor type, and thus represents a variety of tumors and cell types (Supplementary Table S1-S2, see Methods). In general, almost all sialyltransferases were overexpressed, and only rarely underexpressed, across the myriad of human cancers, consistent with hypersialylation often observed (21). However, clear differences in (Supplementary Table S1A) ST8Sia6 expression was observed across different cancers. ST8Sia6 was not significantly underexpressed in any cancer, but ST8Sia6 overexpression varied by 20-fold from just 0.56% in the pancreas to 8.85% in the large intestine or 10.67% in the kidney. Similarly, for any location, the relative overexpression of any sialyltransferase varied. For the large intestine, the highest level of overexpression was observed for ST8Sia6 (Supplementary Table S1B).

Checkpoint blockade has not yet been shown to be effective for the majority of patients with colon cancer (with the exception of rare subtype with microsatellite instability), indicating that other mechanisms of immune evasion may be at play (22). To understand whether ST8Sia6 impacted patient survival, correlation of ST8Sia6 overexpression with patient outcome was examined in the Human Protein Atlas database (https://www.proteinatlas.org). The Human Protein Atlas used optimal difference between survival above (high) and below (low) a certain threshold of RNA expression based on FPKM (See Methods). For a subset of cancers, high expression of ST8Sia6 correlated with poor survival: colon cancer, stomach cancer, cervical cancer and urothelial cancer (Fig. 1A). Thus, high expression of ST8Sia6 in human cancers negatively impact survival.

ST8Sia6 generates ligands for Siglec-7 and Siglec-9

The expression of sialyltransferases was examined in the MC38 colon and B16-F10 melanoma cell lines by qPCR (Supplementary Fig. S1A-B). ST8Sia6 mRNA was not detected in either MC38 or B16-F10 cell lines. We generated MC38 and B16-F10 cell lines that stably expressed myc-tagged ST8Sia6 to parallel the overexpression that occurs in human tumors. Empty vector (EV) plasmids were transfected into the cell lines as controls. Stable expression of ST8Sia6 did not alter the expression of any other sialyltransferase in MC38 or B16-F10 cell lines (Supplementary Fig. S1A-B). As a functional output for stable expression of ST8Sia6, recombinant Siglec-E was used to probe for expression of ligands, as we previously demonstrated that ST8Sia6 generates ligands for Siglec-E (17). ST8Sia6 transfected MC38 and B16-F10 cell lines had increased recombinant Siglec-E binding compared to EV control cell lines (Fig. 1B-C). Minimal binding and no significant changes were detected with recombinant Siglec-7 and Siglec-9 in either the transfected or EV murine cell lines (Fig. 1D-G). Siglec-E exhibited some binding to the B16-F10 EV control without detectable ST8Sia6, indicating that it also recognized the products of other sialyltransferases. Siglec-9 is the closest human paralog to Siglec-E, with Siglec-7 also having homology. The ability of Siglec-9 and Siglec-7 to bind to ST8Sia6-expressing human

HEK293T cells was examined (Fig. 1H-I). Transiently transfected cell lines were examined for expression of myc-tagged ST8Sia6 and cytidine monophospho-N-acetylneuraminic acid hydroxylase (CMAH)(Fig. 1J). CMAH is an enzyme that mediates the generation of N-glycolylneuraminic acid (Neu5Gc) from N-acetylneuraminic acid (Neu5Ac)(23). Human cells do not express a functional CMAH and primarily contain Neu5Ac. Thus, the preferential usage of Neu5Gc and NeuAc in mice and humans, respectively, could influence the binding of Siglecs. We demonstrated that ST8Sia6-expressing HEK293T cells had increased binding of Siglec-7 and Siglec-9 compared to EV controls (Fig. 1H-I). However, when cells were additionally transfected with CMAH, binding to Siglec-7 and Siglec-9 was decreased, indicating that a sialic acid specificity for Neu5Ac was are critical for Siglec-7 and -9 recognition. Lectin binding was also examined in MC38 and B16-F10 using MALII, which has preferential binding to α2,3-disialic acids, and SNBL, which has preferential binding to α2,6-disialic acids (Supplementary Fig. S1C-D). No change was detected in SNBL or MALII binding indicating that there is not a dramatic shift in cell surface sialylation when ST8Sia6 was ectopically expressed.

Stable expression of ST8Sia6 on cancer cells increases tumor growth and reduces survival

To determine the effect of ST8Sia6 expression on tumor growth, syngeneic C57Bl/6 mice were injected subcutaneously with either MC38 or B16-F10 cells that were either EV transfected or stably expressed ST8Sia6. Mice injected with MC38 ST8Sia6 exhibited accelerated tumor growth ($p=0.0035$) and reduced survival ($p=0.0074$) compared to mice injected with MC38 EV controls (Fig. 2A). Similarly, mice injected with B16-F10 ST8Sia6 exhibited accelerated tumor growth ($p=0.0299$) and reduced survival ($p=0.0053$) compared to mice injected with B16-F10 EV controls (Fig. 2B). To determine if this increase in tumor growth was due to a localized effect on the tumor or resulted from a systemic effect on the mouse immune system, mice were challenged with MC38 or B16-F10 in a dual flank model where the EV cell line was injected on the right flank and the ST8Sia6 stable cell line was injected on the left flank (Fig. 2A-B). In both cases, ST8Sia6-overexpressing tumors grew at a faster rate than the EV controls ($p=0.0032$ for MC38 ST8Sia6 tumors and $p=0.0013$ for B16-F10 ST8Sia6 tumors). The acceleration in tumor growth upon ST8Sia6 stable expression could be due to an intrinsic enhancement of proliferation or due to extrinsic factors, such as a negative impact on the immune response. To determine whether there was an intrinsic effect on cell growth due to stable expression of ST8Sia6, the growth rate in culture was examined by CSFE dilution over time (Supplementary Fig. S1E). The growth rate was similar between MC38 or B16-F10 cells in culture with ST8Sia6 expression compared to EV controls. Thus, the increase in tumor growth was not due to an intrinsic change in proliferation.

ST8Sia6 leads to increased tumor growth independently of PD-L1 expression on tumors

Because not all patients respond to anti-PD-1 or anti-PD-L1 checkpoint therapy, ST8Sia6 overexpression may serve as an alternative mechanism by which cancer cells can evade immune detection independent of the PD-1/PD-L1 axis (22). To determine whether the effects of ST8Sia6 were independent of PD-1/PD-L1, PD-L1-deficient MC38 and B16-F10 cell lines were stably transfected with either ST8Sia6 or EV and examined for alterations in

tumor growth in C57Bl/6 syngeneic mice as described above. MC38 PD-L1 KO ST8Sia6 tumors showed accelerated tumor growth (p=0.0014) and reduced survival (p=0.0048) compared to MC38 PD-L1 KO EV controls (Fig. 2C). Similarly, B16-F10 PD-L1 KO ST8Sia6 tumors showed accelerated tumor growth (p=0.0359) and reduced survival (p=0.0075) as compared to B16-F10 PD-L1 KO EV controls (Fig. 2D). In addition, in the dual flank model, there was accelerated growth of MC38 PD-L1 KO ST8Sia6 tumors (p=0.0011) and B16-F10 PD-L1 KO ST8Sia6 tumors (p=0.0071) as compared to controls (Fig. 2C-D). Thus, the increase in tumor growth observed with ST8Sia6 stable expression was independent of PD-L1 expression on the tumor.

Increased cell growth of ST8Sia6-expressing tumors is dependent on host Siglec-E expression

The change in tumor growth observed could be due to a tumor-cell extrinsic effect on the immune response. Previously, we demonstrated that ST8Sia6 generates ligands for Siglec-E (17), which is a negative regulator of immune cell activation. Thus, the enhanced rate of tumor growth by ST8Sia6-expressing tumors may require Siglec-E expression in the host. To test this, C57Bl/6 and Siglec-E KO mice were injected with either MC38 or B16-F10 expressing ST8Sia6 or EV controls. Consistent with previous results above, MC38 ST8Sia6-expressing tumors (blue line) injected into C57Bl/6 mice grew faster ($p<0.0001$) and reduced survival (p=0.0027) compared to MC38 EV tumors (red line, Fig. 3A). However, the growth advantage of ST8Sia6-expressing MC38 was abrogated when injected into Siglec-E KO mice. MC38 ST8Sia6 tumors injected into Siglec-E KO mice (green line) displayed similar growth rates and survival compared to MC38 EV tumors injected into WT mice (red line) or MC38 EV tumors injected into Siglec-E KO mice (orange line). The same abrogation of the growth advantage was observed in ST8Sia6-expressing B16-F10 tumors when injected into Siglec-E KO mice (green line, Fig. 3B). Thus, the enhancement of tumor growth with ST8Sia6 stable expression was not cell-intrinsic, but cell-extrinsic and depended on the expression of Siglec-E in the host.

ST8Sia6 expression does not alter recruitment of immune cells into the tumor microenvironment

Siglec-E is expressed only on hematopoietic cells, including neutrophils, monocytes, macrophages, and dendritic cells (DCs) but not NK cells, whereas there is conflicting evidence on the expression of Siglec-E in T cells (13; 15; 24-26). We examined the expression of Siglec-E in splenic monocytes, classical and hybrid macrophages, neutrophils, classical DCs, and in $CD4^+$ and $CD8^+$ T cells (Supplementary Fig. S2A-C). Siglec-E was expressed on all myeloid cells examined, but not on splenic nor tumor $CD4^+$ or $CD8^+$ T cells (Fig. 4A-B). Siglec-E engagement was previously shown to inhibit neutrophil recruitment to the lungs (24), and thus, one possibility is that ST8Sia6 expression on tumors alters the profile of immune cells entering the tumor microenvironment (TME). However, no differences were observed in the number of myeloid cells or T cells that infiltrated either MC38 or B16-F10 tumors with stable expression of ST8Sia6 compared to EV controls (Fig. 4C-D). The absence of Siglec-E in the host did not alter the infiltration of myeloid cells or T cells into either MC38 or B16-F10 tumors (Fig. 4C-D). Exhaustion markers on $CD8^+$ T-cells was also examined, and no significant differences in expression of LAG3, PD-1, TIM3,

TCF1, or TOX were observed (Supplementary Fig. S2D). There were also no differences observed by gross histology (Supplementary Fig. S3). Therefore, the changes observed with tumor growth and survival with increased expression of ST8Sia6 was not due to differences in the recruitment of immune cells into the TME.

ST8Sia6 expression alters macrophage polarization and Treg proportions within the TME

Tumor-associated macrophages (TAMs) present within the TME develop proinflammatory or suppressive phenotypes, which can either enhance or inhibit an effective immune response to the tumors (27-29). Therefore, we examined whether ST8Sia6 overexpression on tumors could influence the polarization of macrophages. C57Bl/6 and Siglec-E KO mice were injected with either MC38 (EV or ST8Sia6) or B16-F10 (EV or ST8Sia6) tumor cells. After 7 days, tumors were harvested. This time point was chosen because the majority of immune cells are myeloid cells and are representative of the cells in the TME that lymphocytes encounter at entry. TAMs were analyzed for expression of proteins associated with an inflammatory “M1-like” phenotype (CD38, iNOS) or tolerogenic “M2-like” phenotype (CD206, Arg-1). CD38 and iNOS expression on M1 macrophages promote inflammation, while CD206 and Arg-1 expression on M2 macrophage suppress an immune response (30-36). TAMs were categorized into either classical ($CD11c^{-}$) or hybrid ($CD11c^{+}$) macrophages, as defined in Supplementary Figure S2 (37). Hybrid macrophages within ST8Sia6-expressing MC38 and B16-F10 tumors exhibited the greatest change with higher expression of CD206 and Arg-1, and lower expression of CD38 and iNOS compared to the hybrid macrophages within the MC38 EV controls (Fig. 5A, Supplementary Fig. S4A). Classical macrophages within ST8Sia6-expressing MC38 and B16-F10 tumors also exhibited changes in protein expression associated with altered differentiation. In MC38 ST8Sia6-expressing tumors, Arg-1 was increased and iNOS was decreased compared to MC38 EV controls (Fig. 5B). In B16-F10 ST8Sia6-expressing tumors, CD206 and Arg-1 was increased (Fig. 5B). Thus, expression of ST8Sia6 on tumors altered macrophage polarization away from a pro-inflammatory M1-like phenotype and towards a suppressive M2-like phenotype. This increased expression of CD206 and Arg-1 on hybrid macrophages was lost when ST8Sia6-expressing MC38 and B16-F10 were injected into Siglec-E KO mice. Arg-1 expression on other myeloid cell populations was examined, which was also increased by ST8Sia6 expression on tumors (Supplementary Fig. S4B). No significant differences in Siglec-E protein expression were observed in myeloid cells from either EV control or ST8Sia6-expressing tumors (Supplementary Fig. S4C-S4D). Therefore, although the numbers of macrophages within the tumor were similar, expression of ST8Sia6 on tumors changes macrophage polarization towards a suppressive phenotype characterized by increased expression of CD206 and Arg-1, which requires expression of Siglec-E.

Previously, it has been shown that uptake of α2,3 or α2,6 sialylated antigens via Siglec-E on DCs leads to the generation of tolerizing DCs that promote generation of regulatory T cells (Tregs), resultingin tolerance rather than T-cell activation and initiation of an immune response (38). Therefore, expression of ST8Sia6 on tumor cells may also engage Siglec-E to promote Tregs within the tumors. The proportions of Tregs within the $CD4^{+}$ T-cell pool was examined in ST8Sia6-expressing MC38 and B16-F10 tumor cells compared to EV controls at day 14 after inoculation, at which point there was a substantial infiltration of the tumors

by lymphocytes. An increased proportion of Foxp3^{+} Tregs in the CD4^{+} T-cell pool was seen in ST8Sia6-expressing MC38 tumors compared to EV controls (Fig. 5C). The enhanced Treg generation by ST8Sia6-expressing MC38 tumors was abrogated when injected into Siglec-E KO mice. However, there was no significant changes in Treg proportions in B16-F10 tumors (Fig. 5C). CD8/CD4 and CD8/Treg ratios also did not change (Fig. 5D-E). Therefore, ST8Sia6 expression on tumors led to promotion of a suppressive phenotype in macrophages, with upregulation of CD206 and Arg-1, as well as increasedTreg proportion (in the MC38 tumor model), both of which depend on the expression of Siglec-E in the host.

ST8Sia6 accelerates tumorigenesis in a spontaneous tumor model

Using the MC38 and B16-F10 model systems, we demonstrated that stable expression of ST8Sia6 enhanced tumor growth and decreased survival. We next sought to determine whether ST8Sia6 overexpression accelerated tumorigenesis *in vivo*, utilizing the spontaneous colorectal cancer murine model **T**s4-cre **A**PC$^{lox468(fl/wt)}$ LSLK**r**as^{G12D} (abbreviated as “TAR” hereafter)(19; 39). TAR mice develop colon cancer at approximately 6 months of age. We previously generated a mouse model to induce expression of ST8Sia6 in a cre-dependent manner (17). These were interbred with TAR mice to generate **S**T8Sia6 LNL-**t**TA **T**s4-cre **A**PC$^{lox468(fl/wt)}$ LSLK**r**as^{G12D} mice (hereafter abbreviated as “StTAR”). In this system, the expression TS4-cre within StTAR mice induces ectopic ST8Sia6 expression along with expression of oncogenic Kras^{G12D} and truncation of APC. Although TAR mice developed adenomas/adenocarcinomas in the small and large bowel, with a median survival of approximately 6 months, StTAR mice had accelerated tumorigenesis, with a median survival of 67 days (Fig. 6A). The expression of ST8Sia6 alone in the gut (ST8Sia6 LNL-tTA Ts4-cre mice, abbreviated “StT” hereafter) in the absence of any oncogenes did not lead to the development of polyps or cancer, and mice were healthy for up to 18 months (Fig. 6A). At the time of euthanasia, the small bowel and colon were examined for macroscopic growths (Fig. 6B). StTAR mice had extensive lesion formation on both the small bowel and colon, with numbers comparable to that observed in TAR mice, although it should be noted that at the time of endpoint examination, StTAR mice were considerably younger than TAR mice (Fig. 6A). One month old wild-type (WT) and TAR mice had normal colon morphology by histology (Supplementary Fig. S5). However, young StTAR mice had extensive lesion formation, with morphology consistent with adenomas/adenocarcinomas (Supplementary Fig. S5). Histology was performed to examine expression of PCNA and MCM6, which are associated with active proliferation of tumor cells and high αSMA, which is associated with a fibrotic response (Fig. 6C, Supplementary Fig. S5). Lesions that developed in TS4-cre APC$^{lox468(fl/wt)}$ (abbreviated as “TA” hereafter) and TAR mice at experimental endpoints also exhibited increased PCNA, αSMA, and MCM6 but appeared to have reduced Arg-1 staining compared to StTAR mice (Fig. 6C). In one-month old mice, only StTAR, but not TAR, mice had lesions that expressed PCNA, MCM6, and Arg-1 (Supplementary Fig. S5). To quantify changes in Arg-1 expression between TAR and StTAR mice, lesions were microdissected from colons and processed for flow cytometry (Fig. 6D-E). MHCII^{+} and MHCII^{-} hybrid and classical macrophages were analyzed for Arg-1 expression (Fig. 6D-E). MHCII^{+} and MHCII^{-} hybrid macrophages, as well as MHCII^{+} classical macrophages, within tumors had significantly increased Arg-1 protein expression from StTAR compared to TAR mice (Fig. 6D-E, Supplementary S6A). MHCII^{+} and MHCII

⁻ hybrid macrophages, but not classical, also had significantly increased Arg-1 expression in non-tumor colons of StTAR mice compared to TAR mice (Fig. 6D-E). Arg-1 expression was also examined in other myeloid populations (Supplementary Fig. S6B). Significant increases in Arg-1 were also observed in monocytes from StTAR tumors compared to TAR tumors, whereas DCs and neutrophils did not display such differences. Arg-1 expression was also increased in these populations in the colons between StTAR and TAR mice (Supplementary Fig. S6B). No significant differences were observed in Siglec-E expression in StTAR compared to TAR mice in any myeloid population (Supplementary Fig. S6C). Therefore, ST8Sia6 overexpression within an established spontaneous mouse model of colon cancer led to an acceleration in tumorigenesis and decreased survival, demonstrating that increased ST8Sia6 expression had a functional role in tumor development. Thus, mice with cancer cells overexpressing ST8Sia6 (either flank tumors or spontaneous tumors) have increased tumor growth and reduced survival, which is due to modulation of the immune response through Siglec-E (summarized in Fig. 7).

Discussion

Although it has been long-recognized that many tumors have increased incorporation of sialic acids in cell surface glycans, there have been few studies to examine the function of individual sialic transferases in cancer and even less is known about the mechanism(s) of action. Here, we demonstrated that ST8Sia6 expression in tumors led to accelerated tumor growth and alteration of the immune response. Using both MC38 and B16-F10 tumor cells engineered to express ST8Sia6, ST8Sia6 expression led to increased tumor growth in single flank and dual flank models. This increased tumor growth was abrogated when ST8Sia6-expressing MC38 and B16-F10 were injected into Siglec-E KO mice, demonstrating that ST8Sia6 exerts its effects on tumors in a cell-extrinsic manner. Within the TME, engagement of Siglec-E by ST8Sia6-expressing tumors upregulated expression of Arg-1, which functions to inhibit immune responses (34-36). Thus, ST8Sia6 on tumors modulates the function of infiltrating immune cells, which requires Siglec-E. Using a spontaneous mouse model of colon cancer, ST8Sia6 expression accelerated tumorigenesis, decreasing survival to a median of 67 days instead of approximately 6 months in the absence of ST8Sia6 on tumors. Similar to what was observed in MC38 and B16-F10 models, there was increased Arg-1 expression in myeloid cells in colon tumors when ST8Sia6 was overexpressed. Therefore, ST8Sia6 expression accelerates tumor growth and alters immune responses, which is dependent on Siglec-E.

Previously, we demonstrated that ST8Sia6 generates ligands for murine Siglec-E (17), which was confirmed using MC38 and B16-F10 cell lines. Here, we demonstrated that ST8Sia6 also generated ligands for Siglec-7 and Siglec-9. In human cancers, Siglec-9 expression was found in tumor-infiltrating lymphocytes (TILs) from patients with non-small cell lung cancer (NSCLC), colon cancer, and epithelial ovarian cancer (40-41). There was a correlation in NSCLC patients with a higher frequency of Siglec-9-expressing TILs with a worse overall survival (40). Functionally, Siglec-9 engagement also alters macrophage gene expression. Muc1 engagement of Siglec-9 on macrophages leads to an increase in CD206, as well as CD163, which are associated with alternative/M2-like macrophage activation (41). A different group demonstrated that Siglec-9 engagement increases Arg-1 expression on the

macrophage cell line RAW264 (42). Thus, engagement of either Siglec-E on murine macrophages or Siglec-9 on human macrophages both lead to the expression of Arg-1.

Current advances in cancer immunotherapy, including the advent of checkpoint inhibitors that block PD-1/PD-L1 and CTLA-4, have shown that the immune system can be mobilized and manipulated to combat cancer. Although these biologics are a powerful tool in reducing tumor burden and increasing patient survival, there are limitations. Many patients do not respond to checkpoint blockade therapy and, for certain cancers, checkpoint blockade is generally ineffective. In colon cancer, for example, checkpoint blockade was effective in only the 4% of patients with high microsatellite instability (MSI-H) (43). In addition, some patient tumors do not express PD-L1 (B7-H1) (44). Thus, tumors may utilize other mechanisms of immune evasion, including increased sialylation, such as through ST8Sia6 (45). Here, we demonstrated that ST8Sia6 expression on tumors modulated the immune response through Siglec-E, leading to increase in Arg-1 expression on TAMs. The relative contributions of various myeloid populations to enhanced growth by ST8Sia6-expressing tumors awaits the generation and examination of cell-specific Siglec-E conditional knockout mice.

Ectopic expression of ST8Sia6 in the murine MC38 and B16-F10 tumor cell lines led to the generation of ligands for murine Siglec-E, but not human Siglecs-7 and -9. However, humans lack a functional CMAH gene, which catalyzes generation of Neu5Gc from Neu5Ac, leading to differences in sialic acids utilized by humans and as compared to mice (23). To determine whether this was the cause for the lack of Siglec-7 and -9 binding in MC38 or B16-F10 tumor lines, we repeated the experiments using human HEK293T cells. When HEK293T cells were transfected with ST8Sia6, ligands were subsequently generated for Siglecs-7 and -9. To confirm the species difference was responsible, HEK293T cells were co-transfected with CMAH and ST8Sia6. Co-expression of CMAH with ST8Sia6 abrogated the generation of ligands for Siglec-7 and -9, although CMAH co-expression did not alter ST8Sia6 protein expression. Thus, there is a preference for Siglec-7 and Siglec-9 for Neu5Ac as compared to Neu5Gc. Interestingly, it was previously reported that MC38 constitutively expresses ligands for both Siglec-E and Siglec-9 (13). Our results demonstrate that expression of CMAH, as found in murine cells, disrupts generation of ligands for Siglec-9 and that binding of Siglec-E to MC38 tumor cells requires expression of ST8Sia6. This previous group also showed a significant difference in growth of the MC38 tumor cells when injected into Siglec-E KO mice compared to WT mice (13). This may reflect the differences in the presence of Siglec-E ligands on the MC38 cell lines used, as their MC38 has high expression of Siglec-E ligands and ours did not (except when ST8Sia6 was expressed).

In the spontaneous colorectal cancer model, expression of ST8Sia6 accelerates tumorigenesis. Although the number of lesions in both the small bowel and colon of these mice at endpoint are similar, it is important to recognize that the average endpoint for TAR mice was nearly 6 months, whereas the average endpoint for StTAR mice was approximately 67 days. Future studies will examine whether inhibition of ST8Sia6 can slow tumor growth *in vivo*. The StTAR mice were engineered such that cre expression removed the lox-neo-lox cassette controlling expression of the tet transactivator, leading to upregulation of ST8Sia6

expression. This tet transactivator is inhibitable by doxycycline, allowing temporal regulation of ST8Sia6. Thus, although there are currently no inhibitors for ST8Sia6, the use of doxycycline will allow us to analyze the effects of ST8Sia6 inhibition at different points during tumorigenesis in this model, as well as to determine whether decreased ST8Sia6 expression could synergize with checkpoint blockade to slow the growth of colon cancer.

Supplementary Material

Refer to Web version on PubMed Central for supplementary material.

Acknowledgements

We thank Nicoleta Carapanceanu and Valentin Carapanceanu of the Khazaie laboratory for their help in processing and embedding tissue samples for histology. This work was supported by the Mayo Clinic Center of Biomedical Discovery and National Institutes of Health R01CA243545 (to V.S.S.), 2T32AI007425 (to V.S.S. and D.J.F.) and R01AI108682 (to K.K.).

References

1. Gibbons Johnson RM, Dong H. Functional expression of Programmed Death-Ligand 1 (B7-H1) by immune Cells and Tumor Cells. Front Immunol 2017;8:1–9. [PubMed: 28149297]
2. Chamoto K, Hatae R, Honjo T. Current issues and perspectives in PD-1 blockade cancer immunotherapy. Int J of Clin Oncol 2020;25:790–800. [PubMed: 31900651]
3. Wei SC, Duffy CR, Allison JP. Fundamental Mechanisms of Immune Checkpoint Blockade Therapy. Cancer Discov 2018;8:1069–1086. [PubMed: 30115704]
4. Jaiswal S, Jamieson CHM, Pang WW, Park CY, Chao MP, Majeti R, et al. CD47 is upregulated on circulating hematopoietic stem cells and leukemia cells to avoid phagocytosis. Cell 2009;138:271–285. [PubMed: 19632178]
5. Pathria P, Louis TL, Varner JA. Targeting Tumor-Associated Macrophages in Cancer. Trends Immunol 2019;40:310–327. [PubMed: 30890304]
6. Kumar V, Patel S, Tcyganov E, Gabrilovich DI. The Nature of Myeloid-Derived Suppressor Cells in the Tumor Microenvironment. Trends Immunol 2016;37:208–220. [PubMed: 26858199]
7. Läubli H, Varki A. Sialic acid-binding immunoglobulin-like lectins (Siglecs) detect self-associated molecular patterns to regulate immune responses. Cell Mol Life Sci 2020;77:593–605. [PubMed: 31485715]
8. van de Wall S, Santegoets KCM, van Houtum EJH, Büll C, Adema GJ. Sialoglycans and Siglecs Can Shape the Tumor Immune Microenvironment. Trends Immunol 2020;41:274–285. [PubMed: 32139317]
9. Duan S, Paulson JC. Siglecs as Immune Cell Checkpoints in Disease. Annu Rev Immunol 2020;38:365–395. [PubMed: 31986070]
10. Macauley MS, Crocker PR, Paulson JC. Siglec-mediated regulation of immune cell function in disease. Nat Rev Immunol 2014;14:653–666. [PubMed: 25234143]
11. Barkal AA, Brewer RE, Markovic M, Kowarsky M, Barkal SA, Zaro BW, et al. CD24 signalling through macrophage Siglec-10 is a target for cancer immunotherapy. Nature 2019;572:392–396. [PubMed: 31367043]
12. Wang J, Sun J, Liu LN, Flies DB, Nie X, Toki M, et al. Siglec-15 as an immune suppressor and potential target for normalization cancer immunotherapy. Nat Med 2019;25:656–666. [PubMed: 30833750]
13. Läubli H, Pearcea OMT, Schwarza F, Siddiquia SS, Denga L, Stanczaka MA, Denga L, Verhagena A, Secresta P, Luskb C, Schwartzb AG, Varkia NM, Buic JD, and Varkia A. Engagement of myelomonocytoic Siglecs by tumor-associated ligands modulates the innate immune response to cancer. PNAS 2014;111:14211–14216. [PubMed: 25225409]

14. Gray MA, Stanczak MA, Mantuano NR, Xiao H, Pijnenborg JFA, Malaker SA, et al. Targeted glycan degradation potentiates the anticancer immune response in vivo. Nat Chem Biol 2020;Online ahead of print.
15. Zhang JQ, Biedermann B, Nitschke L, Crocker PR. The murine inhibitory receptor Siglec-E is expressed broadly on cells of the innate immune system whereas mSiglec-F is restricted to eosinophils. Eur J Immunol 2004;34:1175–1184. [PubMed: 15048729]
16. Teintenier-Lilievre M, Julien S, Juliant S, Guerardel Y, Duonor-Cérutti M, Delannoy P, et al. Molecular cloning and expression of human hST8SiaVI (alpha 2,8 sialyltransferase) responsible for the synthesis of the diSia motif on O-glycoproteins. Biochem J 2005;392:665–674. [PubMed: 16120058]
17. Belmonte PJ, Shapiro MJ, Rajcula MJ, McCue SA, Shapiro VS. Cutting Edge: ST8Sia6-Generated α-2,8-Disialic Acids Mitigate Hyperglycemia in Multiple Low-Dose Streptozotocin-Induced Diabetes. The J Immunol 2020;204:3071–3076. [PubMed: 32350083]
18. Tang H, Liang Y, Anders RA, Taube JM, Qiu X, Mulgaonkar A, et al. PD-L1 on host cells is essential for PD-L1 blockade– mediated tumor regression. J Clin Invest 2018;128:580–588. [PubMed: 29337303]
19. Saadalla AM, Osman A, Gurish MF, Dennis KL, Blatner NR, Pezeshki A, et al. Mast cells promote small bowel cancer in a tumor stage-specific and cytokine-dependent manner. PNAS 2018;115:1588–1592. [PubMed: 29429965]
20. Beard C, Hochedlinger K, Plath K, Wutz A, Jaenisch R. Efficient method to generate single-copy transgenic mice by site-specific integration in embryonic stem cells. Genesis 2006;44:23–28. [PubMed: 16400644]
21. Rodrigues E, Macauley MS. Hypersialylation in Cancer: Modulation of Inflammation and Therapeutic Opportunities. Cancers (Basel) 2018;10:1–19.
22. Yaghoubi N, Soltani A, Ghazvini K, Hassanian SM, Hashemy SI. PD-1/ PD-L1 blockade as a novel treatment for colorectal cancer. Biomed Parmacother 2019;110:312–318.
23. Hedlund M, Tangvoranuntakul P, Takematsu H, Long JM, Housley GD, Kozutsumi Y, et al. N-glycolylneuraminic acid deficiency in mice: implications for human biology and evolution. Mol Cell Biol 2007;27:4340–4346. [PubMed: 17420276]
24. McMillan MJ, Sharma RS, McKenzie EJ, Richards HE, Zhang J, Prescott A, et al. Siglec-E is a negative regulator of acute pulmonary neutrophil inflammation and suppresses CD11b β2-integrin–dependent signaling. Blood 2013;121:2084–2094. [PubMed: 23315163]
25. Büll C, Boltje TJ, Balneger N, Weischer SM, Wassink M, van Gemst JJ, et al. Sialic Acid Blockade Suppresses Tumor Growth by Enhancing T-cell-Mediated Tumor Immunity. Cancer Res 2018;78:3574–3588. [PubMed: 29703719]
26. Nagala M, McKenzie E, Richards H, Sharma R, Thomson S, Mastroeni P, et al. Expression of Siglec-E Alters the Proteome of Lipopolysaccharide (LPS)-Activated Macrophages but Does Not Affect LPS-Driven Cytokine Production or Toll-Like Receptor 4 Endocytosis. Front Immunol 2018;8:1–17.
27. Qian B, Pollard JW. Macrophage diversity enhances tumor progression and metastasis. Cell 2010;141:39–51. [PubMed: 20371344]
28. Gabrilovich DI, Ostrand-Rosenberg S, Bronte V. Coordinated regulation of myeloid cells by tumours. Nat Rev Immunol 2012;12:253–268. [PubMed: 22437938]
29. Tcyganov E, Mastio J, Chen E, Gabrilovich DI. Plasticity of myeloid-derived suppressor cells in cancer. Curr Opin Immunol 2018;51:76–82. [PubMed: 29547768]
30. Jablonski KA, Amici SA, Webb LM, de Dios Ruiz-Rosado J, Popovich PG, Partida-Sanchez S, et al. Novel markers to delineate murine M1 and M2 macrophages. PLoS One 2015;10:1–25.
31. Amici SA, Young NA, Narvaez-Miranda J, Jablonski KA, Arcos J, Rosas L, et al. cD38 is robustly induced in human Macrophages and Monocytes in inflammatory conditions. Front Immunol 2018;9:1–13. [PubMed: 29403488]
32. Matalonga J, Glaria E, Bresque M, Escande C, María Carbó J, Kiefer K, et al. The Nuclear Receptor LXR Limits Bacterial Infection of Host Macrophages through a Mechanism that Impacts Cellular NAD Metabolism. Cell Rep 2017;18:1241–1255. [PubMed: 28147278]

33. Fan W, Yang X, Huang F, Tong X, Zhu L, Wand S. Identification of CD206 as a potential biomarker of cancer stem-like cells and therapeutic agent in liver cancer. Oncol Lett 2019;18:3218–3226. [PubMed: 31452799]
34. Rodriguez PC, Quiceno DG, Zabaleta J, Ortiz B, Zea AH, Piazuelo MB, et al. Arginase I production in the tumor microenvironment by mature myeloid cells inhibits T-cell receptor expression and antigen-specific T-cell responses. Cancer Res 2004;64:5839–5849. [PubMed: 15313928]
35. Rodriguez PC, Zea AH, DeSalvo J, Culotta KS, Zabaleta J, Quiceno DG, et al. L-arginine consumption by macrophages modulates the expression of CD3 zeta chain in T lymphocytes. J Immunol 2003;171:1232–1239. [PubMed: 12874210]
36. Kusmartsev S, Nefedova Y, Yoder D, Gabrilovich DI. Antigen-specific inhibition of CD8+ T cell response by immature myeloid cells in cancer is mediated by reactive oxygen species. J Immunol 2004;172:989–999. [PubMed: 14707072]
37. Sheng J, Chen Q, Soncin I, Ng SL, Karjalainen K, Ruedl C. A Discrete Subset of Monocyte-Derived Cells among Typical Conventional Type 2 Dendritic Cells Can Efficiently Cross-Present. Cell Rep 2017;21:1203–1214. [PubMed: 29091760]
38. Perdicchio M, Ilarregui JM, Verstege MI, Cornelissen LAM, Schetters STT, Engels S, et al. Sialic acid-modified antigens impose tolerance via inhibition of T-cell proliferation and de novo induction of regulatory T cells. PNAS 2016;113:3329–3334. [PubMed: 26941238]
39. Gounari F, Chang R, Cowan J, Guo Z, Dose M, Gounaris E, et al. Loss of adenomatous polyposis coli gene function disrupts thymic development. Nat Immunol 2005;6:800–809. [PubMed: 16025118]
40. Stanczak MA, Siddiqui SS, Trefny MP, Thommen DS, Boligan KF, von Gunten S, et al. Self-associated molecular patterns mediate cancer immune evasion by engaging Siglecs on T cells. J Clin Invest 2018;128:4912–4923. [PubMed: 30130255]
41. Beatson R, Tajadura-Ortega V, Achkova D, Picco G, Tsourouktsoglou T, Klausing S, et al. The mucin MUC1 modulates the tumor immunological microenvironment through engagement of the lectin Siglec-9. Nat Immunol 2016;17:1273–1283. [PubMed: 27595232]
42. Higuchi H, Shoji T, Murase Y, Iijima S, Nishijima K. Siglec-9 modulated IL-4 responses in the macrophage cell line RAW264. Biosci Biotechnol Biochem 2016;80(3):501–509. [PubMed: 26540411]
43. Boland PM, Ma WW. Immunotherapy for Colorectal Cancer. Cancers 2017;9:1–12.
44. Kim JM, Chen DS. Immune escape to PD-L1/PD-1 blockade: seven steps to success (or failure). Ann Oncol 2016;27:1492–1504. [PubMed: 27207108]
45. Kalathil SG, Thanavala Y. High immunosuppressive burden in cancer patients: A major hurdle for cancer immunotherapy. Cancer Immunol Immunother 2016;65:813–819. [PubMed: 26910314]

Synopsis

Expression of sialyltransferase ST8Sia6 by tumor cells generates ligands that bind to Siglec-E on macrophages, resulting in their repolarization to an M2-like phenotype. The data highlight the potential targeting of ST8Sia6 to enhance antitumor responses.

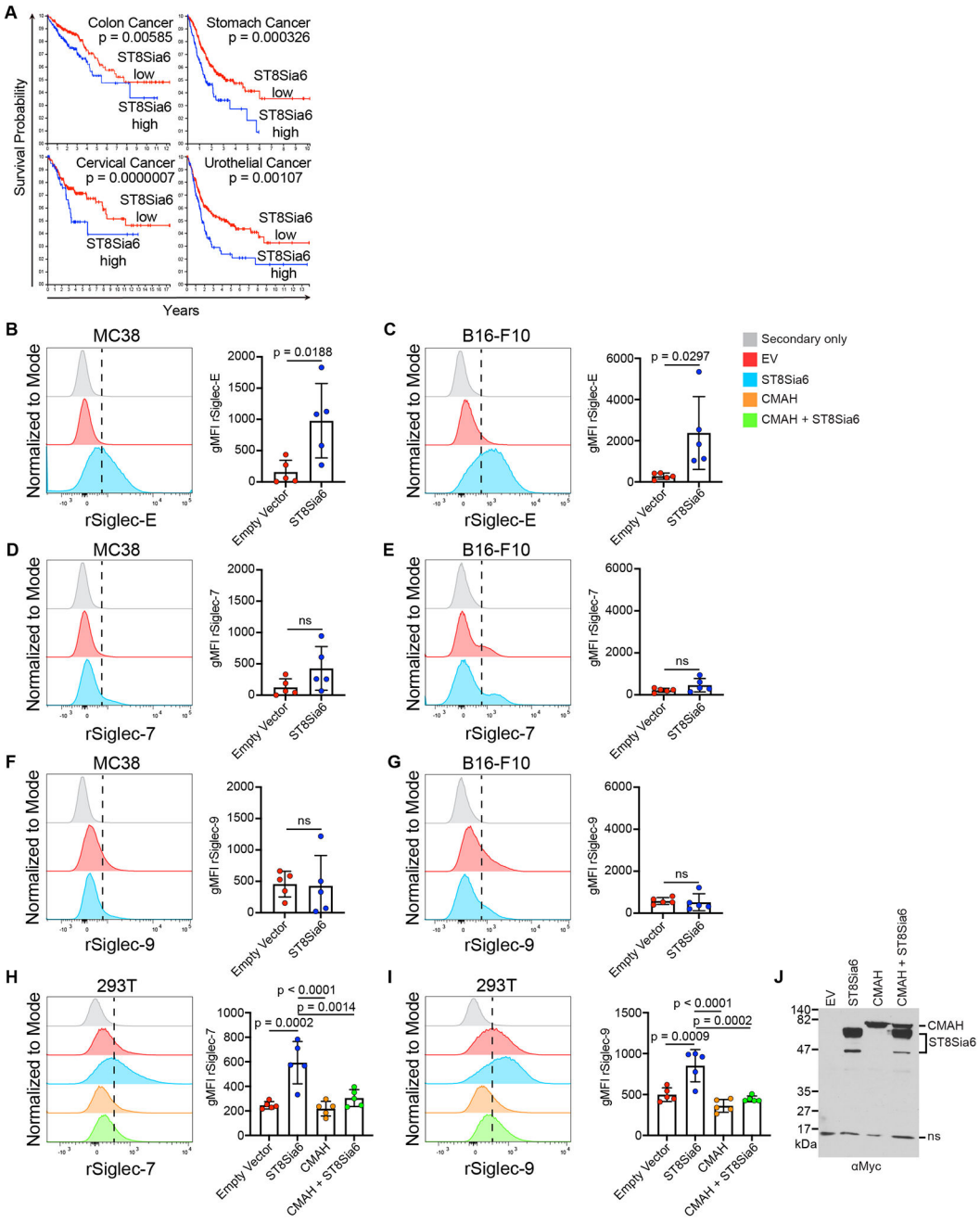

Fig. 1. ST8Sia6 Overexpression in Human Cancers and Generation of Ligands for Siglec-E, Siglec-7, and Siglec-9.

(**A**) Survival data from the Human Protein Atlas for selected human cancers that had high (blue line) or low (red line) ST8Sia6 expression is shown. Colon cancer used a threshold of 0.2 FPKM to separate low (n=353) and high (n=244) expressers. Stomach Cancer used a threshold of 0.3 FPKM to separate low (n=267) and high (n=67) expressers. Cervical Cancer used a threshold of 0.2 FPKM to separate low (n=255) and high (n=66) expressers. Urothelial cancer used a threshold of 0.1 FPKM to separate low (n=310) and high (n=96) expressers. (**B-G**) MC38 and B16-F10 murine cancer cell lines were stably transfected with

either ST8Sia6-Myc or an empty vector (EV) control and were probed for ligands with recombinant (**B**, **C**) Siglec-E, (**D**, **E**) Siglec-7, and (**F**, **G**) Siglec-9 by flow cytometry. (**H**, **I**) HEK293T cells were transiently transfected with ST8Sia6-Myc or empty vector, with or without CMAH. Ligands for (**H**) Siglec-7 and (**I**) Siglec-9 were probed by flow cytometry using recombinant Siglec-7 or -9. (**B**-**I**) gMFI was quantified across 5 independent experiments, and significance analyzed by one-way ANOVA between groups. ns, not significant. (**J**) Lysates from (**H**, **I**) were examined for expression of CMAH-myc and ST8Sia6-myc by Western blotting for the myc-tag.

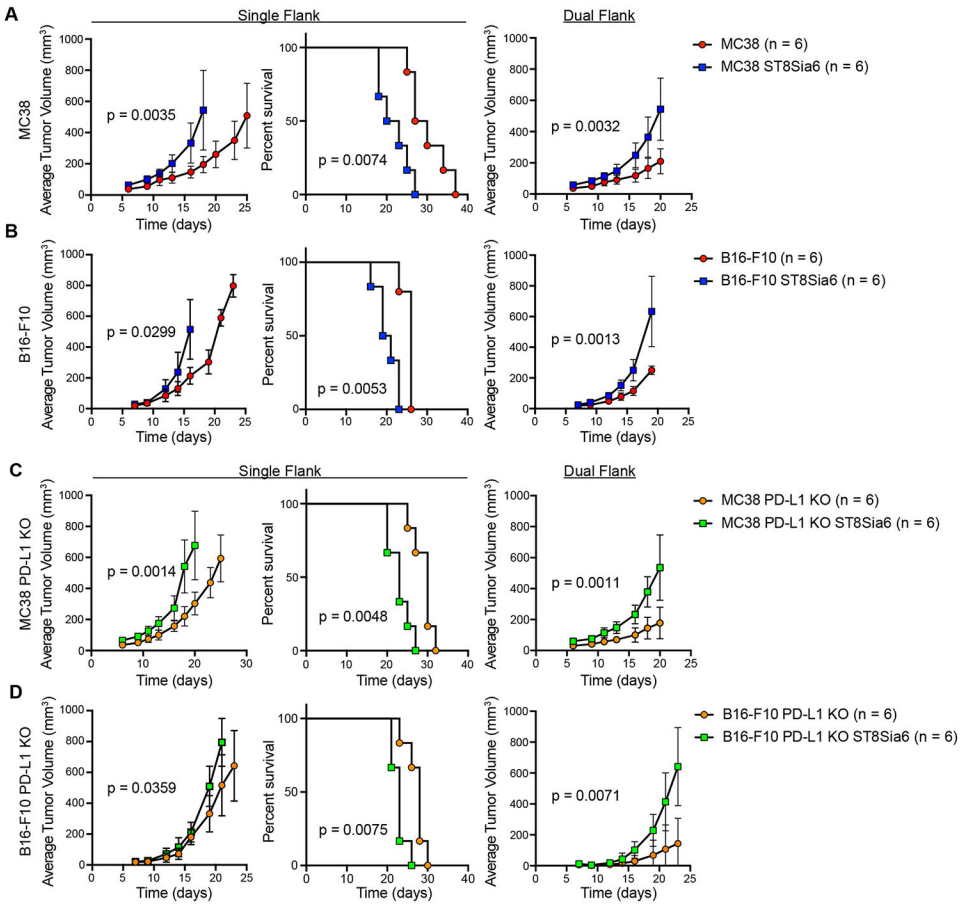

Fig. 2. ST8Sia6 Overexpression Increases Tumor Growth and Reduces Survival in a PD-L1-Independent Manner.

MC38 and B16-F10 were either transfected with ST8Sia6-Myc or an empty vector (EV) control. (**A**) MC38 or (**B**) B16-F10 cancer cells (EV or ST8Sia6-Myc stably transfected) and (**C**) MC38 PD-L1 KO or (**D**) B16-F10 PD-L1 KO cancer cells (EV or ST8Sia6-Myc stably transfected) were injected subcutaneously into the flank of C57Bl/6 mice. Tumor growth and survival were assessed for single flank injections, whereas tumor growth was evaluated for dual flank injections. 6 mice were analyzed per group. Survival was compared using a Mantel-Cox test. Differences in tumor growth kinetics were analyzed using a two-way ANOVA across all timepoints. P-values were generated when all mice were present within each group.

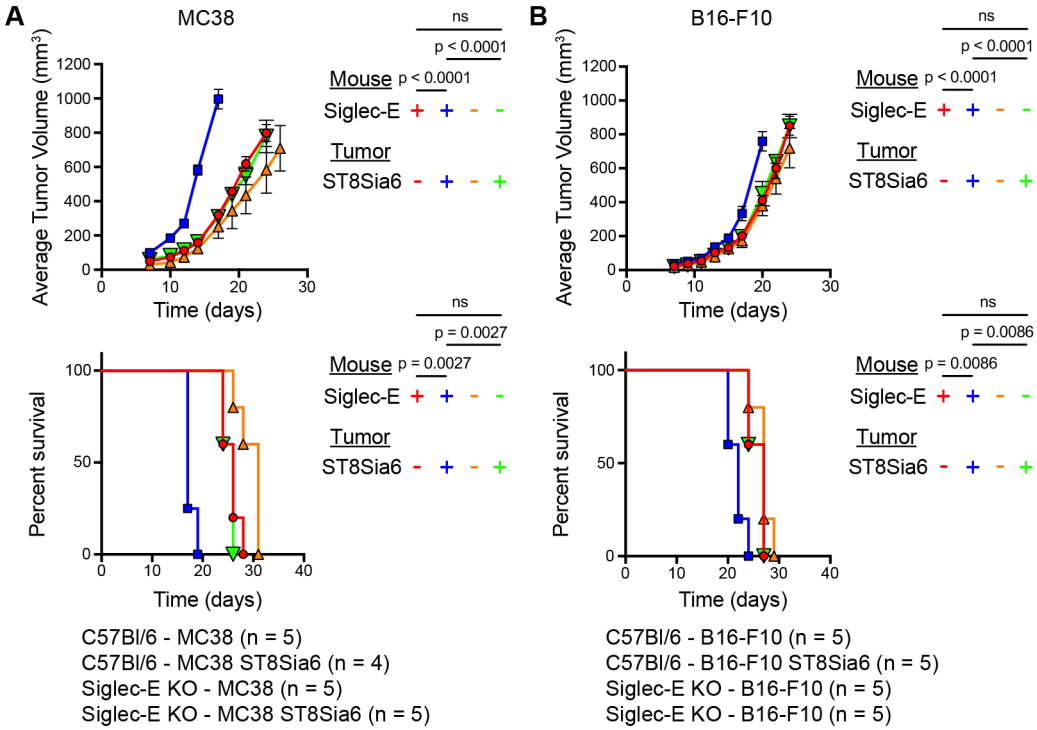

Fig. 3. ST8Sia6 Overexpression Increases Tumor Growth and Reduces Survival in a Siglec-E-Dependent Manner.

C57Bl/6 WT or Siglec-E KO mice were injected with either (**A**) MC38 or (**B**) B16-F10 cancer cells (empty vector or ST8Sia6-Myc stably transfected) on the right flank. Tumor growth and survival was assessed. 4-5 mice were analyzed per group. Survival was compared using a Mantel-Cox test. Differences in tumor growth kinetics between groups were analyzed using a two-way ANOVA across all timepoints. P-values were generated when all mice were present within each group. ns, not significant.

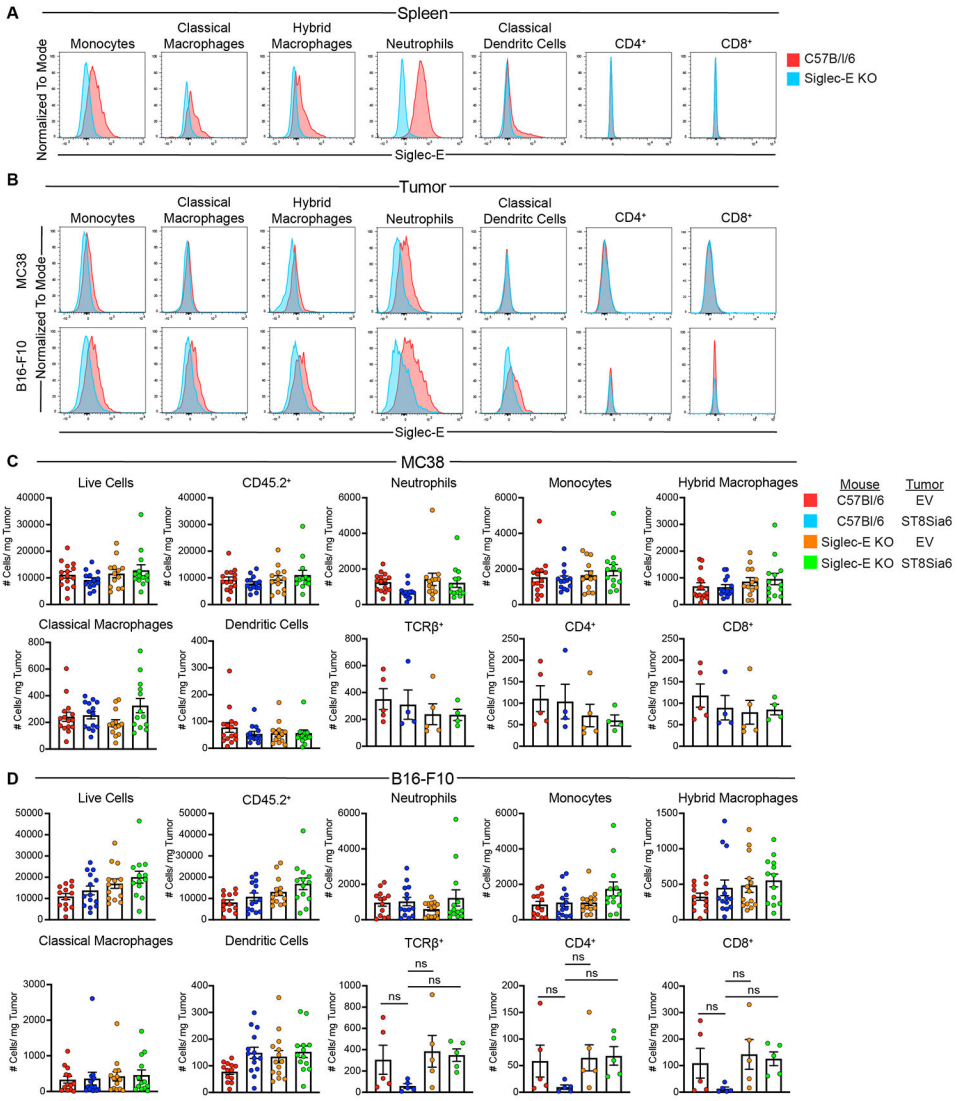

Fig. 4. Analysis of Tumor-Infiltrating Immune Cells in MC38 and B16-F10 Models.

(**A**) Siglec-E expression was examined on monocytes, classical macrophages, hybrid macrophages, neutrophils, classical dendritic cells, $CD4^+$, and $CD8^+$ T cells from WT and Siglec-E KO splenocytes from adult mice. (B) C57Bl/6 WT or Siglec-E KO mice were injected with either MC38 or B16-F10 cancer cells. Tumors were harvested on day 7 (myeloid cells) or day 14 (T-cells) and analyzed using flow cytometry. (**C-D**) C57Bl/6 WT or Siglec-E KO mice were injected with either (**C**) MC38 or (**D**) B16-F10 cancer cells (EV or ST8Sia6-Myc stably transfected) on the right flank. Tumors were harvested on day 7 (myeloid cells) or day 14 (T-cells) and analyzed using flow cytometry. Myeloid cells (n=12-15 mice) and T cells (n=4-5 mice) were analyzed. The number of cells per mg tumor was quantified for live $CD45.2^+$ neutrophils, monocytes, hybrid macrophages, classical macrophages, dendritic cells, $TCR\beta^+$ cells, and $CD4^+$ and $CD8^+$ T cells. Statistics were performed using a one-way ANOVA between groups. ns, not significant.

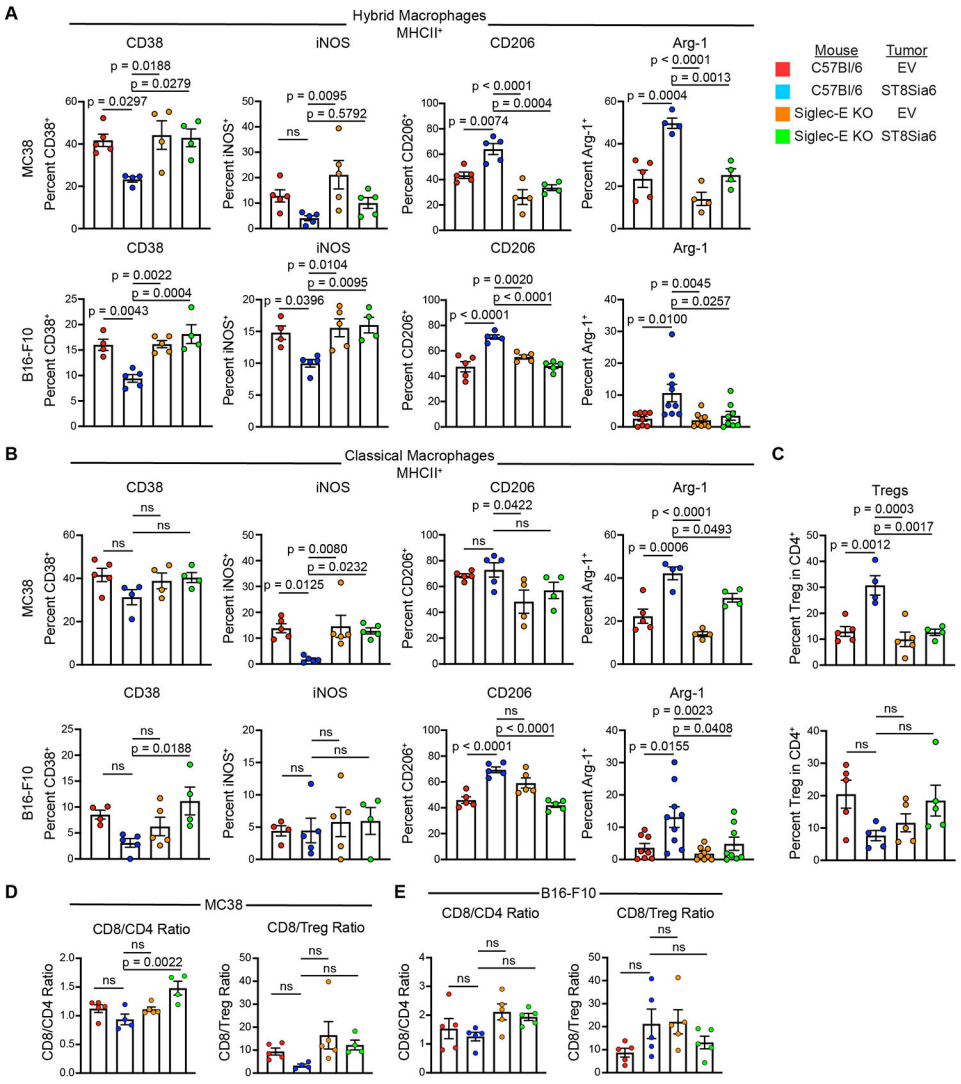

Fig. 5. ST8Sia6 Overexpression Induces TAMs to Exhibit a Suppressive M2-like Phenotype.

MC38 or B16-F10 cancer cells (EV or ST8Sia6-Myc stably transfected) were injected on the right flank of C57Bl/6 or Siglec-E KO mice. Tumors were harvested at day 7 for TAM analysis or day 14 for T-cell analysis using flow cytometry. 4-5 mice were analyzed per group for macrophage polarization and Tregs. TAMs were defined as $MHCII^+$ (**A**) hybrid ($CD11c^+$) or (**B**) classical ($CD11c^-$) macrophages and were analyzed for expression of CD38, iNOS, CD206, and Arg-1 by flow cytometry. Frequencies of $CD38^+$, $iNOS^+$, $CD206^+$, and Arg-1^+ TAMs were quantified. (**C**) Frequencies of $Foxp3^+CD25^+$ Tregs within the $CD4^+TCR\beta^+$ T-cell pool was quantified. (**D**) Intratumoral CD8/CD4 and CD8/Treg ratios were examined. Statistics were performed using a one-way ANOVA between groups. ns, not significant.

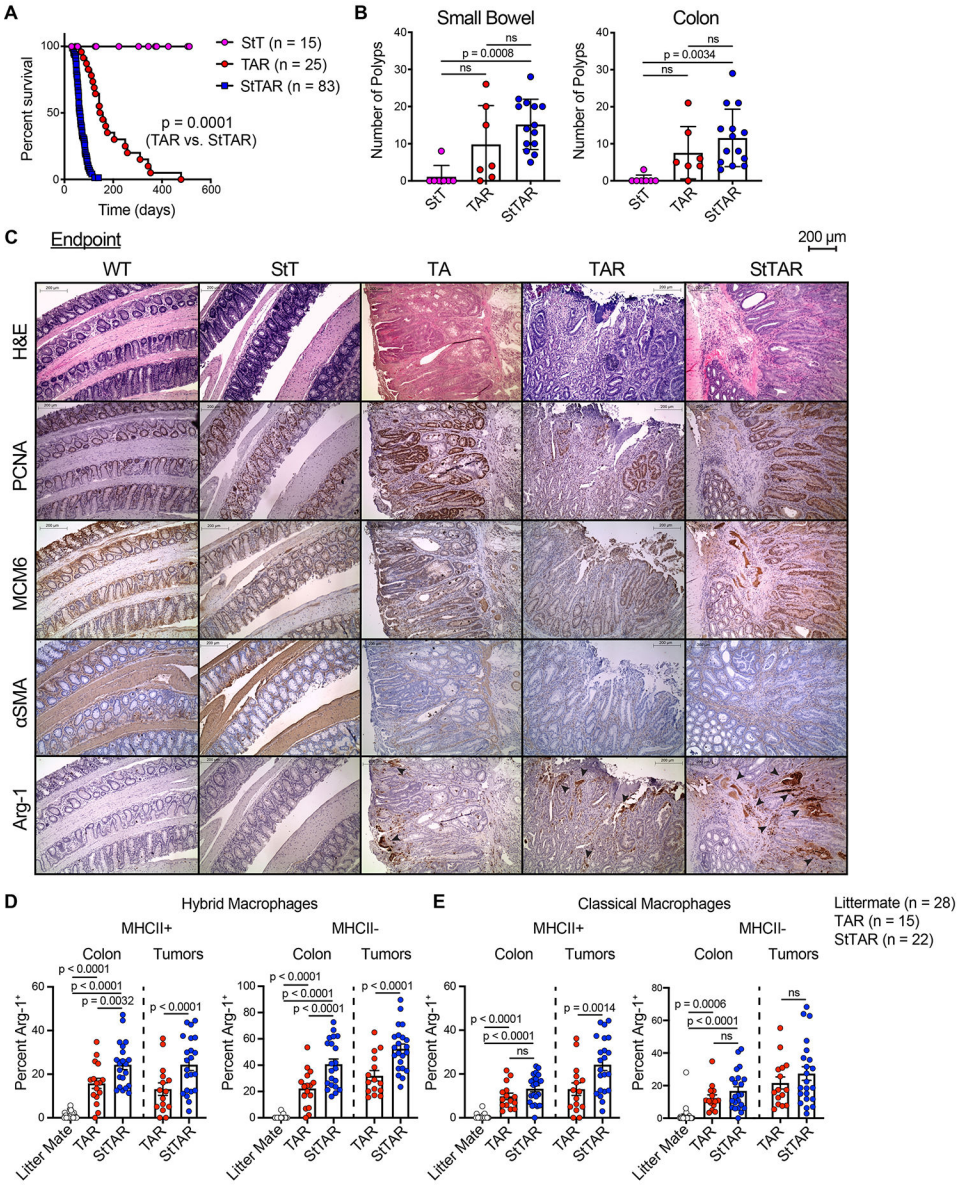

Fig. 6. Accelerated Tumorigenesis, Reduced Survival, and Increased Arg-1 Expression on TAMs is observed when ST8Sia6 is Overexpressed in a Spontaneous Colon Cancer Model.

(**A**) Survival data on TAR (Ts4-cre $APC^{lox468(fl/wt)}$ $LSLKRas^{G12D}$), StTAR (ST8Sia6 LNL-tTA Ts4-cre $APC^{lox468(fl/wt)}$ LSL $KRas^{G12D}$), and StT (ST8Sia6 LNL-tTA Ts4-cre) mice. P values between curves were calculated using a two-way ANOVA between groups. (**B**) Number of macroscopic lesions in the small bowel or colon of StT, TAR and StTAR mice at endpoint. (**C**) H&E staining for adenomas/adenocarcinoma expression of PCNA, MCM6, αSMA, and Arg-1 in mice of the indicated genotypes, as noted above the histology. Ages of the mice shown are as follows: WT (366 days), StT (391 days), TA (246 days), TAR (142 days), and StTAR (59 days). Arrows denote areas of Arg-1 staining. Arg-1 expression was quantified from (**D**) hybrid and (**E**) classical macrophages comparing colon from littermate, and colon and tumors TAR and StTAR mice. Statistics were performed using a one-way ANOVA between groups. ns, not significant.

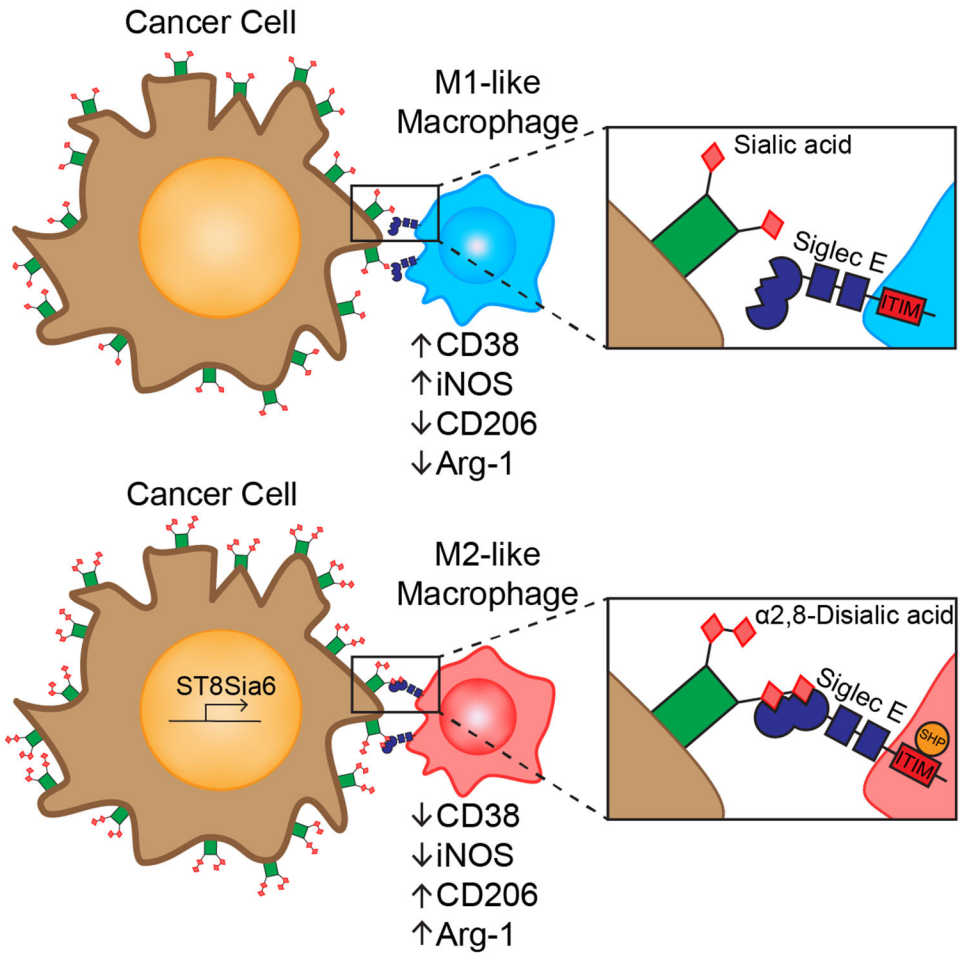

Fig. 7. Model of ST8Sia6 Overexpression in Cancer and the Interaction with the Siglec-E on Macrophages.

When ST8Sia6 is upregulated in murine cancer cells, sialic acids on glycoproteins are modified to α2,8-disialic acids, which have preferential binding to Siglec-E on macrophages and other innate immune cells. Siglec-E activation leads to activation of intracellular ITIM domains that recruit SHP proteins and leads to a shift in TAM polarization towards an M2-like phenotype.